

# Progenitor B-1 B-cell acute lymphoblastic leukemia is associated with collaborative mutations in 3 critical pathways

Sheryl M. Gough,<sup>1,\*</sup> Liat Goldberg,<sup>1,\*</sup> Marbin Pineda,<sup>1</sup> Robert L. Walker,<sup>1</sup> Yuelin J. Zhu,<sup>1</sup> Sven Bilke,<sup>1</sup> Yang Jo Chung,<sup>1</sup> Joseph Dufraine,<sup>1</sup> Subhadip Kundu,<sup>1</sup> Elad Jacoby,<sup>2</sup> Terry J. Fry,<sup>2</sup> Susanna Fischer,<sup>3</sup> Renate Panzer-Grümayer,<sup>3,4</sup> Paul S. Meltzer,<sup>1</sup> and Peter D. Aplan<sup>1</sup>

<sup>1</sup>Genetics Branch and <sup>2</sup>Pediatric Branch, Center for Cancer Research, National Cancer Institute, National Institutes of Health, Bethesda, MD; <sup>3</sup>Leukemia Biology Group, Children's Cancer Research Institute, Vienna, Austria; and <sup>4</sup>Department of Pediatrics, Medical University of Vienna, Vienna, Austria

## Key Points

- An NUP98-PHF23 fusion collaborates with acquired Bcor and Jak/Stat mutations to produce a pro-B-1 ALL.
- Gene expression profile of murine pro-B-1 ALL resembles that of a subset of human ALL, suggesting some human ALLs arise from pro-B-1 B cells.

B-1 and B-2 lymphocytes are derived from distinct developmental pathways and represent layered arms of the innate and adaptive immune systems, respectively. In contrast to a majority of murine B-cell malignancies, which stain positive with the B220 antibody, we discovered a novel form of B-cell leukemia in *NUP98-PHF23* (*NP23*) transgenic mice. The immunophenotype (Lin<sup>-</sup> B220<sup>-</sup> CD19<sup>+</sup> AA4.1<sup>+</sup>) was identical to that of progenitor (pro) B-1 cells, and V<sub>H</sub> gene usage was skewed toward 3' V regions, similar to murine fetal liver B cells. Moreover, the gene expression profile of these leukemias was most similar to that of fetal liver pro-B fraction BC, a known source of B-1 B cells, further supporting a pro-B-1 origin of these leukemias. The *NP23* pro-B-1 acute lymphoblastic leukemias (ALLs) acquired spontaneous mutations in both *Bcor* and Janus kinase (*Jak*) pathway (*Jak1/2/3* and *Stat5a*) genes, supporting a hypothesis that mutations in 3 critical pathways (stem-cell self-renewal, B-cell differentiation, and cytokine signaling) collaborate to induce B-cell precursor (BCP) ALL. Finally, the thymic stromal lymphopoietin (Tslp) cytokine is required for murine B-1 development, and chromosomal rearrangements resulting in overexpression of the TSLP receptor (*CRLF2*) are present in some patients with high-risk BCP-ALL (referred to as *CRLF2r* ALL). Gene expression profiles of *NP23* pro-B-1 ALL were more similar to that of *CRLF2r* ALL than non-*CRLF2r* ALL, and analysis of V<sub>H</sub> gene usage from patients with *CRLF2r* ALL demonstrated preferential usage of V<sub>H</sub> regions used by human B-1 B cells, leading to the suggestion that this subset of patients with BCP-ALL has a malignancy of B-1, rather than B-2, B-cell origin.

## Introduction

A wide spectrum of B-cell malignancies has been recognized in humans. These malignancies are typically classified based on the presumed cell of origin and span the breadth of B-cell development, from immature B cells, such as progenitor (pro)-B cells, precursor (pre)-B cells, and pre-pro-B cells, to the more mature B cells, such as plasma cells. A variety of diagnostic tools, including clinical presentation, histology, immunophenotype, cytogenetics, and molecular genetics, have been used to characterize and classify these B-cell malignancies. However, even with these modern tools, a proportion of leukemias and lymphomas remain difficult to classify and are termed leukemias of ambiguous lineage or B-cell lymphoma, unclassifiable.<sup>1</sup>

Submitted 26 June 2017; accepted 2 August 2017. DOI 10.1182/bloodadvances.2017009837.

\*S.M.G. and L.G. contributed equally to this work and should be considered joint first authors.

The full-text version of this article contains a data supplement.

Normal B-cell differentiation is thought to follow 1 of 2 developmental B-cell pathways, designated B-1 and B-2. B-2 B cells constitute the predominant class of B cells found in the spleen, lymph nodes, and peripheral blood and function in adaptive immunity (reviewed by Montecino-Rodriguez and Dorshkind<sup>2</sup>). B-1 B cells are rarely identified in the spleen or lymph nodes but instead predominate in the pleural and peritoneal cavities and are thought to represent an arm of the innate immune system. As such, they produce natural antibodies, which are not induced by exposure to foreign antigens, and typically recognize self-glycosylated and heavily glycosylated antigens. B-1 B cells have been more clearly defined and characterized in mice than in humans and are more prominent during fetal hematopoiesis than during adult hematopoiesis.<sup>2</sup> A unique differentiation pathway for murine B-1 B cells has been characterized, with pro-B-1 cells in the murine fetal liver or bone marrow displaying a lineage negative (Lin<sup>-</sup>) B220 (CD45R)<sup>lo/-</sup> CD19<sup>+</sup> AA4.1<sup>+</sup> immunophenotype.<sup>3,4</sup> Defining B-1 B cells in humans has been challenging, but human B-1 B cells have been described as CD3<sup>-</sup> CD19<sup>+</sup> CD20<sup>+</sup> CD27<sup>+</sup> CD43<sup>+</sup> CD69<sup>-</sup> CD70<sup>-</sup>, distinguishing them from naïve and memory B cells (CD43<sup>-</sup>), plasmablasts/plasma cells (CD19<sup>lo</sup>CD20<sup>lo/-</sup>CD138<sup>±</sup>), CD43<sup>+</sup>-activated B cells (CD69<sup>+</sup>CD70<sup>++</sup>), and T cells (CD3<sup>+</sup>CD19<sup>-</sup>CD20<sup>-</sup>).<sup>5</sup> In addition to their distinctive immunophenotype, umbilical cord B-1 B cells showed a skewed usage of V<sub>H</sub> chains, with preferential usage of V<sub>H</sub>3-30.<sup>5</sup>

Some mature B-cell malignancies, including cases of chronic lymphocytic leukemia in humans<sup>6-8</sup> and CH lymphomas in mice,<sup>9</sup> are suspected to arise from B-1 B cells, and expanded B-1 cell populations have been described in patients with systemic lupus erythematosus.<sup>10</sup> Although B-1 lymphocytes can be transformed by transduction of a *BCR-ABL* retrovirus,<sup>11</sup> leukemias of pro-B-1 B cells arising in genetically engineered mice have not been described. Herein we report that B-cell leukemias that arise in *NUP98-PHF23* (*NP23*) transgenic mice<sup>12</sup> originate from pro-B-1 B cells. Interestingly, these pro-B-1 B-cell leukemias (pro-B-1 ALLs) also acquire somatic mutations in *Bcor* and the Janus kinase (*Jak*) pathway; mutations in these genes have previously been implicated in acute myeloid leukemia (AML),<sup>13</sup> myelodysplastic syndrome,<sup>14</sup> and BCP-ALL.<sup>15,16</sup>

## Materials and methods

Additional information on methods can be found in the supplemental Methods.

### Mice

*NP23* transgenic mice were generated as previously described.<sup>12</sup> *E2a:PBX1* and *E $\mu$ -RET* samples were obtained from spleens of C57BL/6 or BALB/C mice injected with cell lines derived from *E2a:PBX1*<sup>17</sup> or *E $\mu$ -RET*<sup>18</sup> transgenic mice, respectively. All animal studies were approved by the National Cancer Institute Intramural Animal Care and Use Committee.

### Human samples

Samples containing  $\geq 90\%$  blasts were obtained from the Austrian study center upon institutional review approval and with approval of the ethics committee. Informed consent for tissue banking and research studies was obtained from patients, their parents, and/or their legal guardians in accordance with the Declaration of Helsinki.

## Statistics

Continuous variables were compared using an unpaired 2-tailed Student *t* test statistic. A 2 $\times$ 2 contingency table and  $\chi^2$  test with Yates' correction was used to analyze V<sub>H</sub> region utilization.

## Results

### *NP23* mice develop a B220<sup>-</sup> B-lineage ALL

We recently reported that *NUP98-PHF23* (*NP23*) transgenic mice develop acute leukemia with almost complete penetrance by 14 months of age; a diagram of the transgene, which uses *Vav1* regulatory elements<sup>19</sup> to direct transgene expression to the hematopoietic compartment, is provided in Figure 1A.<sup>12</sup> In the initial cohort of mice studied, we detected leukemia in 40 progeny of the B10 founder and 37 progeny of the C10 founder, as well as in 6 additional founder mice.<sup>12</sup> Although most mice developed myeloid or T-cell ALL, 1 mouse (founder I2) developed a BCP-ALL with the immunophenotype of a typical BCP-ALL: CD19<sup>+</sup>B220<sup>+</sup>sIgm<sup>-</sup> (Figure 1B-C). Flow cytometry showed a complete lack of normal Mac1<sup>+</sup>/Gr1<sup>+</sup> myeloid cells in the bone marrow and complete replacement with CD19<sup>+</sup>B220<sup>+</sup> B cells; spleen, lymph node, and thymus also showed invasion of CD19<sup>+</sup>B220<sup>+</sup> B cells (Figure 1C). These findings were confirmed by immunohistochemistry showing complete effacement of the bone marrow with B220<sup>+</sup> cells (Figure 1D). Comparison with a standard scheme for B-cell differentiation (Figure 1B)<sup>20</sup> showed that these cells had matured to at least the fraction BC stage of differentiation, because they had acquired CD19. The diagnosis of B-lineage ALL was further supported by the presence of clonal *Igh* gene rearrangements (supplemental Figure 1).

However, several mice subsequently developed B-lineage leukemia that could not be classified using this standard scheme for B-cell differentiation.<sup>20</sup> An example of 1 such animal, #752, is shown in Figure 1E-F. Flow cytometry (supplemental Figure 2 provides an example of gating strategy) of bone marrow, lymph node, spleen, and thymus showed marked invasion of a uniform CD19<sup>+</sup>/B220<sup>-</sup> population; close inspection of the flow cytometry profile (Figure 1E) revealed a separate CD19<sup>+</sup>/B220<sup>+</sup> population (presumably from residual nonleukemic B cells), indicating that there was not a technical problem with the B220 antibody.

Immunohistochemical analyses supported the flow cytometry findings, revealing invasion and destruction of the normal splenic architecture by cells that were B220<sup>-</sup> and CD3<sup>-</sup> (Figure 1F). Follicle remnant staining with B220 and CD3 can be seen. The CD19<sup>+</sup>B220<sup>-</sup> immunophenotype was puzzling; because standard models of murine B-cell differentiation show that B220 expression precedes CD19 expression (Figure 1B),<sup>20</sup> all CD19<sup>+</sup> cells should also be B220<sup>+</sup>. This phenomenon was not an oddity present in a single sample; 6 additional mice from the original cohort displayed this CD19<sup>+</sup>/B220<sup>-</sup> phenotype (Figure 1G; Table 1). In sum, a total of 7 B-lineage ALLs with a CD19<sup>+</sup>/B220<sup>-</sup> phenotype were identified in our initial cohort, a frequency of 6 of 40 and 1 of 37 for the B10 and C10 *NP23* founder lines, respectively (Table 1). Coincidentally, 2 of the 7 cases (#758 and #1534) had a concurrent precursor T-cell (pre-T) lymphoblastic lymphoma/leukemia (LBL) characterized by a distinct CD4<sup>+</sup>/CD8<sup>+</sup> population in addition to the B-lineage ALL; we previously observed a similar phenomenon in *NP23* mice, which had concurrent AML and pre-T LBL.<sup>12</sup>

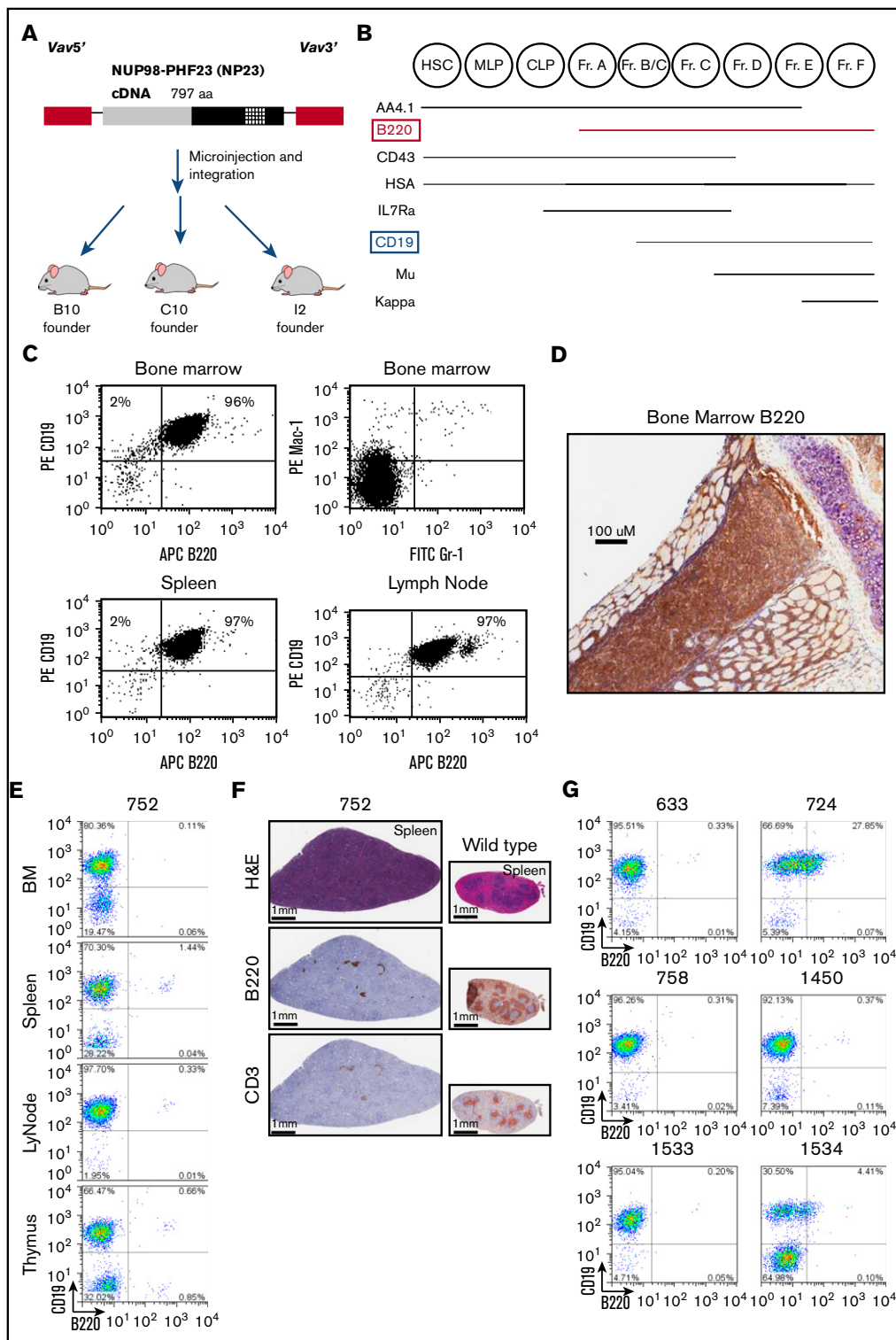


**Figure 1. A subset of *NP23* mice develop a CD19<sup>+</sup> B220<sup>-</sup> leukemia.** (A) Schematic of the *NP23* transgene. *Vav5'* and *3'* regulatory elements are indicated in red, the *NUP98* portion of the transgene is gray, and the *PHF23* portion is black, with the *PHD* domain indicated with crosshatches. (B) Schematic of murine bone marrow (BM) B-lymphopoietic differentiation stages, adapted from Hardy and Hayakawa.<sup>20</sup> (C) Flow cytometry profile of I2 mouse BM, spleen, and lymph node, stained with the indicated antibodies. (D) Immunohistochemical staining of I2 BM with B220 antibody. (E) Representative flow cytometry profiles of BM, spleen, lymph node (LyNode), and thymus from NP-23 B-lineage ALL 752 using CD19 and B220 antibodies. (F) Hematoxylin and eosin (H&E), B220, and CD3 immunohistochemistry of infiltrated 752 spleen compared with a wild-type (WT) control. (G) B220/CD19 cell populations in additional pro-B-1 ALL samples. Analysis shown is of tissues with the highest purity of malignant cells: 633 BM, 724 BM, 758 BM, 1450 BM, 1533 LyNode, and 1534 BM. CLP, common lymphoid progenitor; Fr, fraction; HSC, hematopoietic stem cell; MLP, multilineage progenitor.

**Table 1. NP23 B-lineage ALL characteristics**

ID	Age, mo	Sex	Malignant immunophenotype	Infiltrated tissues	Peripheral blood CBC			
					WBC, ×10 <sup>9</sup> /L	HgB, g/dL	MCV, fL	PLT, ×10 <sup>9</sup> /L
633	8.5	F	B220 <sup>-</sup> /CD19 <sup>+</sup> /AA4.1 <sup>+</sup>	BM, Spl, Liv, Kid	9.7	3.3	59.1	225
724	7.75	F	B220 <sup>lo/-</sup> /CD19 <sup>+</sup> /AA4.1 <sup>+</sup>	BM, Spl, LyNo, Thy, Liv, Kid	102.9	4.8	67.3	202
752	5.75	M	B220 <sup>-</sup> /CD19 <sup>+</sup> /AA4.1 <sup>+</sup>	BM, Spl, LyNo, Thy, Liv, Kid	135.7	10.5	53.8	714
758	10	F	B220 <sup>-</sup> /CD19 <sup>+</sup> /AA4.1 <sup>+</sup> CD4 <sup>+</sup> /CD8 <sup>+</sup> *	BM, Spl, LyNo Thy	78.9	6.9	64.8	153
1450†	9	F	B220 <sup>-</sup> /CD19 <sup>+</sup>	BM, Spl, LyNo	34.84	7.1	87.5	92
1533	7	F	B220 <sup>-</sup> /CD19 <sup>+</sup> /AA4.1 <sup>+</sup>	BM, Spl, LyNo, Liv	nt			
1534	7.5	F	B220 <sup>lo/-</sup> /CD19 <sup>+</sup> /AA4.1 <sup>+</sup> CD4 <sup>+</sup> /CD8 <sup>+</sup> *	BM, Spl, LyNo, Thy, Liv, Kid BM, Spl, LyNo, Thy, Liv, Kid	nt			

BM, bone marrow; CBC, complete blood count; F, female; HgB, hemoglobin; Kid, kidney; Liv, liver; LyNo, lymph node; M, male; MCV, mean corpuscular volume; nt, not tested; Spl, spleen; Thy, thymus; WBC, white blood cell.

\*These 2 mice had concurrent pre-T LBL.

†C10 line.

Given that the B220 antibody reacts with a specific glycosylated isoform of CD45 (*CD45RABC*),<sup>21</sup> we looked for evidence of this isoform. In all but 1 of the B220<sup>-</sup> samples, the B220 splice species was either absent or markedly reduced (supplemental Figure 3), supporting the observation that these samples do not stain for the B220 isoform of CD45. Of note, the sample that did display abundant levels of the *CD45 RABC* messenger RNA (#724) showed a heterogeneous staining with B220 (Figure 1F), leading us to consider these B220<sup>-</sup> B-lineage ALLs could be classified as B220<sup>lo/-</sup>. Overall, we were still left with the puzzling observation that these leukemias were predominantly B220<sup>-</sup>/CD19<sup>+</sup> and thus did not follow the standard differentiation scheme for murine B-cell differentiation (Figure 1B).

A pro-B-1 B lymphocyte has been identified with the immunophenotype B220<sup>lo/-</sup>CD19<sup>+</sup>AA4.1<sup>+</sup>CD43<sup>+</sup>,<sup>4</sup> leading us to speculate that the B-lineage leukemias we were studying might be pro-B-1 leukemias. Additional staining demonstrated that the malignant cells were negative for common lineage markers including Gr1, CD3, CD4, CD8, Ter119, IgM, and CD11b (Mac1); positive for AA4.1 and CD43; and heterogeneous for Il7ra (Figure 2A-B; Table 1). Il7ra pairs with Crlf2 to form the receptor for thymic stromal lymphopoietin (Tslp), a cytokine that stimulates proliferation of pro-B-1 cells (reviewed by Montecino-Rodriguez and Dorshkind<sup>2</sup>). Consistent with the possibility that these leukemias were of pro-B-1 origin, we found these leukemias expressed *Crlf2* using real-time quantitative polymerase chain reaction (PCR) and flow cytometry assays (supplemental Figure 4).

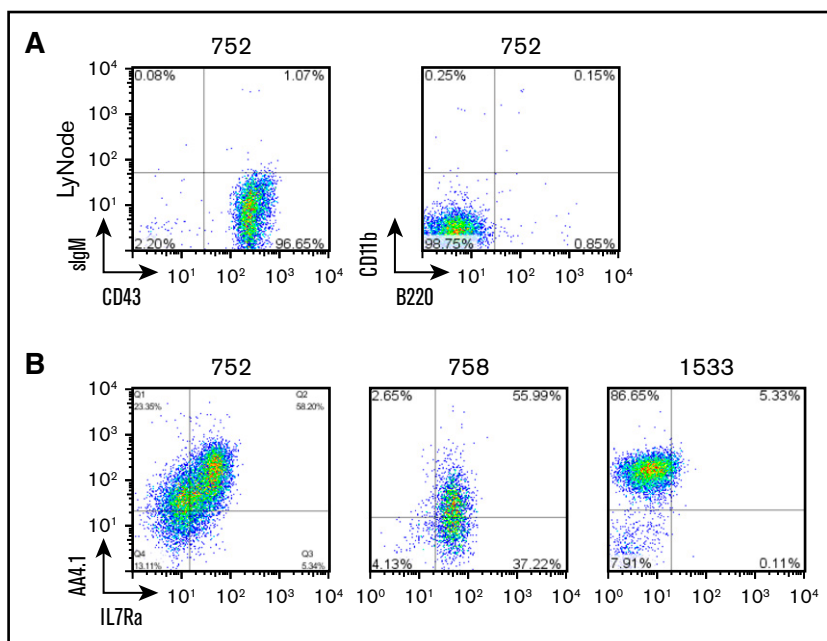


**Figure 2. NP23 B-lineage ALLs display features consistent with pro-B-1 cells.** (A) NP23 ALL sample 752 stained with indicated antibodies. (B) Samples 752, 758, and 1533 stained with AA4.1 and IL7Ra. LyNode, lymph node.

## NP23 B-lineage ALLs show gene expression signatures similar to those of fetal liver pro B cells

We used gene expression profiles to better characterize these leukemias. Analysis of gene expression arrays from the NP23 B-lineage ALL identified 946 probe sets that were >2-fold overexpressed in NP23 B-lineage ALL compared with WT spleen (GSE54787; supplemental Table 1). Comparison of this gene set with a reference set of gene expression profiles derived from a wide spectrum of purified murine B-cell populations (ImmGen) revealed 4 discrete groups: mature B cells, germinal center B cells, common or mixed lymphoid progenitors, and committed pro- or pre-B cells (supplemental Figure 5A). To confirm the expression array data, we used RNA sequencing (RNA-seq) to identify a set of 646 genes that were >2-fold overexpressed in NP23 B-lineage leukemia compared with WT pro- and pre-B cells (fetal liver CD19<sup>+</sup> B220<sup>+</sup> cells; supplemental Table 2). Comparison of this data set with the ImmGen expression arrays again revealed the same 4 groups (supplemental Figure 5B). A total of 106 genes were >2-fold overexpressed in both the expression array and RNA-seq comparisons; these are designated NP23 leukemia core genes (supplemental Table 3).

Hierarchical clustering of the NP23 leukemia core genes revealed that the population most similar to the NP23 B-lineage leukemias were fetal liver fraction BC pro B cells; these cells have previously been shown to be precursors for B-1 lymphocytes<sup>22</sup> (Figure 3A). Gene set enrichment analysis (GSEA) demonstrated enrichment of the NP23 B-lineage leukemia gene signature in fetal liver fraction BC compared with bone marrow fraction BC (Figure 3B); of note, pro-B-1 cells are known to be enriched in fetal liver compared with bone marrow.<sup>22</sup> We next compared the NP23 leukemia core genes identified by combined expression array and RNA-seq with independent, recently described expression profiles of purified pro-B-1 and pro-B-2 cells<sup>23</sup>; GSEA analysis showed that the NP23 B-lineage leukemia gene signature was enriched in pro-B-1 compared with pro-B-2 cells (Figure 3C).

## NP23 B-lineage ALLs preferentially use 3' V<sub>H</sub> genes

All of the pro-B-1 ALL samples showed clonal *Igh* gene rearrangements by southern blot analysis or PCR (supplemental Figures 1 and 6). We investigated the use of *Igh* V<sub>H</sub>, D<sub>H</sub>, and J<sub>H</sub> gene families in these samples by sequencing PCR-amplified VDJ rearrangements. V<sub>H</sub> gene sequences were identified using GenBank accession number BN000872.1 as a reference<sup>24</sup> and D segments as reported by Ye<sup>25</sup> (supplemental Table 4). Samples 758 and 1534 had 1 clonal DJ rearrangement and 2 clonal VDJ rearrangements, indicating that there was subclonal heterogeneity within the tumor cell populations. Mouse 758 had 2 clonal VDJ rearrangements that showed an identical DJ junction but distinct VD junctions, suggesting clonal evolution after transformation and expansion of a cell that had undergone a DJ rearrangement. The V<sub>H</sub> regions used showed a clear bias toward use of 3' V<sub>H</sub> gene families; a similar bias has previously been seen in fetal liver B-1 cells<sup>2,26</sup> (supplemental Figure 6).

We conclude that these B220<sup>lo/-</sup>/CD19<sup>+</sup> leukemias originated from an immature B cell similar to the BCP LBL defined in the Bethesda proposals.<sup>27</sup> However, given that 1) the Lin<sup>-</sup>/B220<sup>lo/-</sup>/CD19<sup>+</sup>/AA4.1<sup>+</sup> immunophenotype matches that of a progenitor B-1 cell, 2) the gene expression profile is more similar to that of

pro-B-1 cells than any other hematopoietic cell type, and 3) the leukemic clones used 3' V<sub>H</sub> regions, we suggest that these leukemias be distinguished from previously defined BCP LBLs and given the designation pro-B-1 ALL.

## Spontaneous *Bcor* mutations occur in pro-B-1 ALL

We suspected that acquisition of spontaneous, collaborative mutations was required for malignant transformation of the NP23 pro-B-1s and used whole-exome sequencing (WES) to screen for mutations in 11 NP23 pro-B-1 ALL samples (the 7 described in Table 1 from the initial cohort, plus 4 identified subsequently). Remarkably, WES revealed that all 11 samples had acquired indel (insertion/deletion) mutations leading to the introduction of premature stop codons and truncation of the BCL6 interacting corepressor (*Bcor*) protein (Figure 4A-B; supplemental Table 5). Of note, 6 of 11 mutations occurred within an 11-bp palindromic hotspot within exon 8 (Figure 4A-B), suggesting an unusual sequence that may be prone to DNA double-strand breaks. Mutations were validated by Sanger sequencing PCR products (Figure 4C). *Bcor* is located on chromosome X; however, only the mutant *Bcor* allele was expressed in all 5 pro-B-1 ALLs examined (Figure 4D).

The premature stop codons encode a truncated *Bcor* protein that retains the BCL6 interaction domain and a portion of the AF9 binding domain but lacks the ankyrin repeats and the PCGF Ub-like fold discriminator (PUFD) domain (Figure 4E). We were unable to detect a truncated *Bcor* protein in the mutant samples, despite using 2 independent anti-*Bcor* antibodies (ab135801 and BCOR 186) that recognized epitopes upstream of the mutation hotspot (supplemental Figure 7), suggesting that the mutant protein may be unstable. Indeed, even when artificially overexpressed in 293T cells, only a faint band representing the truncated protein could be detected (supplemental Figure 7). However, it also may be that *Bcor* expression is below the limit of detection of the antibodies in B cells, because we did not detect *Bcor* protein in WT spleen either. We also examined 16 NP23 AML samples for *Bcor* mutations using WES; in contrast to the high frequency of *Bcor* mutations in the pro-B-1 leukemias, all 16 AML samples were germline for *Bcor*.<sup>28</sup> In addition, WES of the single pre-B-2 ALL sample from the NP23 colony (founder I2) revealed no *Bcor* mutation.

## Jak/Stat pathway activation is associated with pro-B-1 ALL

In addition to acquired *Bcor* mutations, spontaneous mutations of *Jak1*, *Jak2*, or *Jak3* were identified by WES and validated by Sanger sequencing in 7 of the 11 samples (supplemental Table 5). WES variant allele frequency suggested a homozygous *Jak1* mutation in sample 724 and heterozygous mutations in the others. Sample 633 had a *Jak2* point mutation with a variant allele frequency of 14%, suggesting that this was a subclonal progression event. Three of the *Jak* mutations resided within the kinase catalytic domain, whereas the other 5 lay within the pseudokinase domain, a regulatory region that directly binds the catalytic domain and controls its activation.<sup>29</sup> The V657F mutation is similar to the V658F mutation in the pseudokinase domain of *JAK1* identified in patients with high-risk BCP-ALL or Down syndrome BCP-ALL,<sup>16,30-32</sup> and the Y651H mutation is similar to the Y652H mutation found in patients with T-cell ALL.<sup>33,34</sup> The *JAK* V658F mutation has been reported to

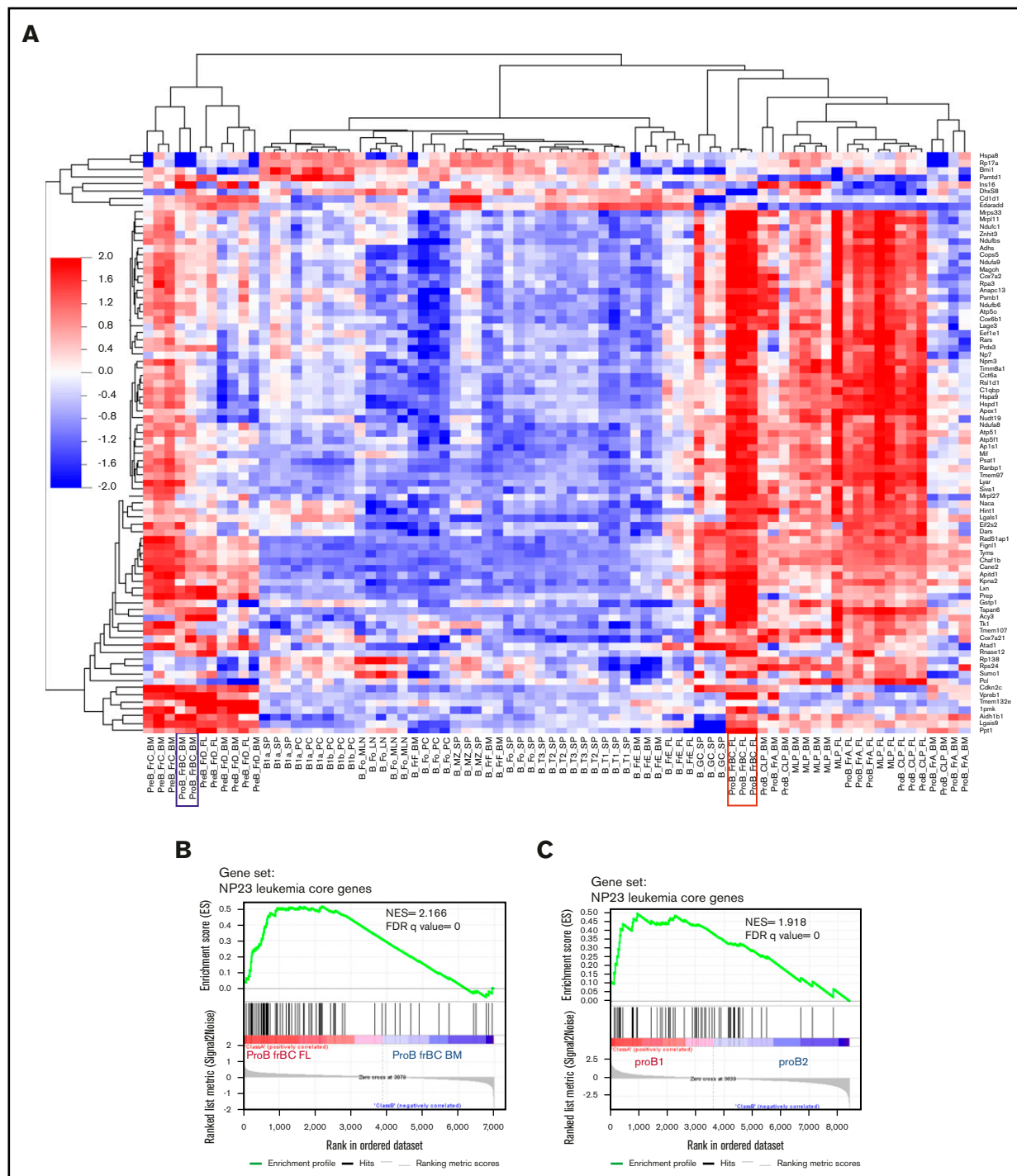


**Figure 3. NP23 B-lineage leukemia gene signature is enriched in fetal liver fraction BC and pro-B-1 cells.** (A) Heat map shows clustering of 106 NP23 leukemia core genes (>2-fold upregulated in NP23 B-lineage leukemias) in expression array data from isolated B-cell populations (GSE15907). Fetal liver (FL) fraction (Fr) BC profile is boxed in red; bone marrow (BM) fraction BC profile is boxed in blue. (B) GSEA plot showing enrichment of NP23 leukemia core upregulated genes in FL Fr BC compared with BM Fr BC (GSE15907). (C) Enrichment of NP23 leukemia core upregulated genes in pro-B-1 vs pro-B-2 cells<sup>23</sup> (GSE81411). FDR, false-discovery rate; LN, lymph node; MLN, mesenteric LN; NES, normalized enrichment score; PC, peritoneal cavity; SP, spleen.

result in constitutive activation of STAT3 and STAT5,<sup>35</sup> suggesting the involvement of the JAK/STAT signaling pathway (reviewed by Vainchenker and Constantinescu<sup>36</sup>) in the etiology of these pro-B-1 ALLs. Moreover, 1 of the 4 samples that lacked a *Jak* mutation

(#1533) had acquired a *Stat5a* missense mutation. Phosphorylation of Stat5 was present, and phosphorylated Stat3 (pStat3) was moderately increased as well (supplemental Figure 8). Of note, sample 1533, which showed the most dramatic Stat5

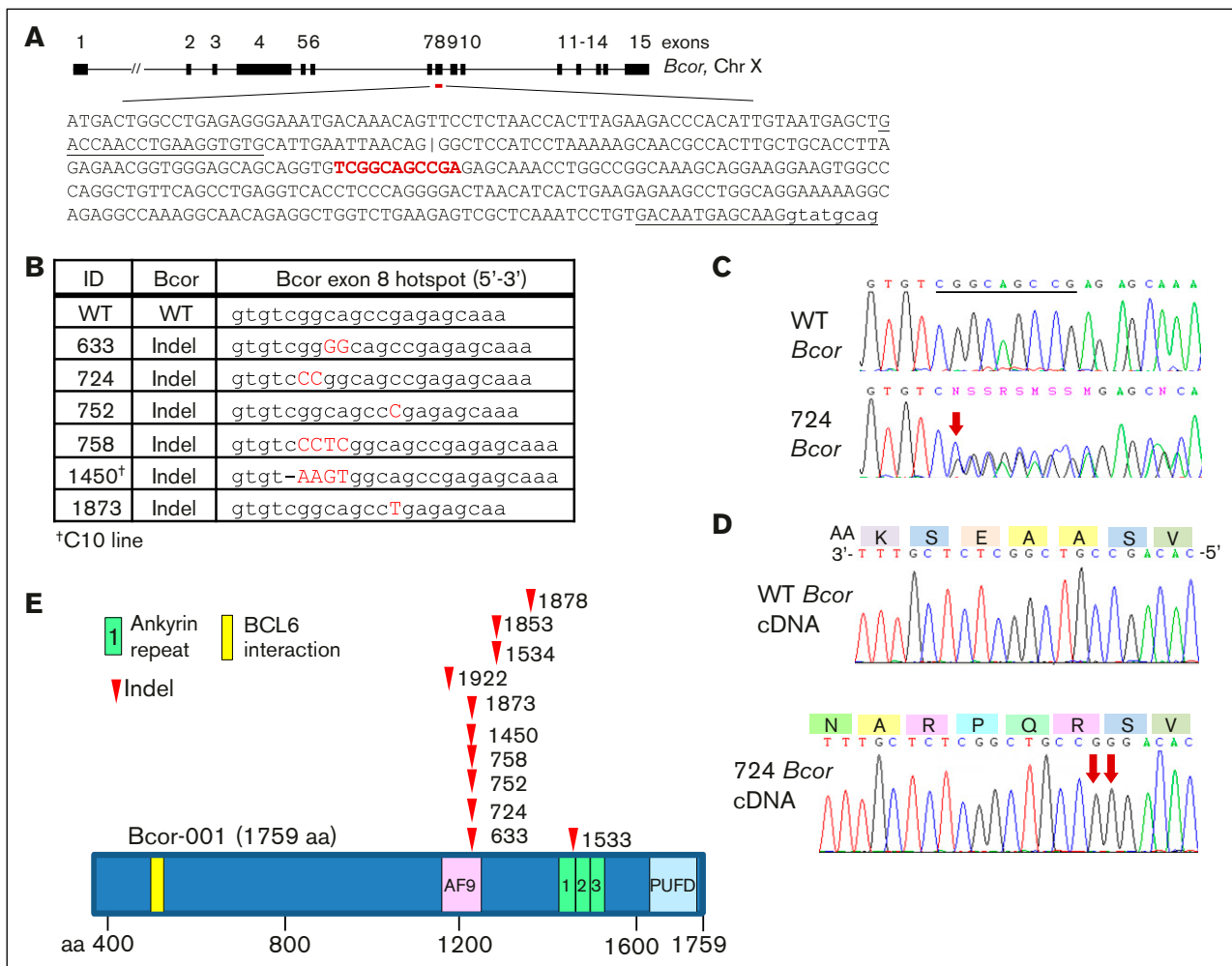


**Figure 4. Bcor mutations in NP23 pro-B-1 ALL.** (A) Schematic of mouse *Bcor* transcript (Bcor-001; ENSMUST00000115513), exons 1 to 15. Black upper-case text is exon 8 coding sequence. Underlined sequence indicates PCR primers. An internal alternative exon 8 splice acceptor site is indicated (||). The *Bcor* 11-bp palindromic mutational hotspot is shown in red. (B) *Bcor* exon 8 mutations at the exon 8 hotspot; indels shown in red capital letters. (C) WT and 724 pro-B-1 ALL sequence across the mutational hotspot (underlined). Red arrow indicates site of CC dinucleotide insertion. (D) 724 messenger RNA expression (lower panel). Red arrows indicate CC dinucleotide insertion. Predicted amino acid sequence is indicated (upper panel). (E) Schematic of the mouse *Bcor* protein and mutation sites (arrowheads).

phosphorylation, did not have a *Jak* mutation but did have an acquired *Stat5a* mutation (supplemental Table 3).

### Patients with BCP-ALL and *CRLF2* overexpression have a gene expression profile similar to that of NP23 pro-B-1 ALL and preferentially use B-1 lymphocyte V<sub>H</sub> segments

Of note, *JAK1/2* mutations in patients with BCP-ALL often occur in the context of aberrant *CRLF2* expression,<sup>37,38</sup> similar to the *Jak1/2* mutations and *Crfl2* expression that we have observed in the murine pro-B-1 ALLs. The association of *JAK1/2* mutation and *CRLF2* activation, along with the observation that murine pro-B-1s are dependent on the *Crfl2* ligand (Tslp),<sup>4</sup> leads to the intriguing hypothesis that some patients with BCP-ALL may have an ALL of B-1, as opposed to B-2, origin. We used RNA-seq to compare the gene expression profile of 2 murine pre-B-2 ALL models (CD19<sup>+</sup>B220<sup>+</sup>CD22<sup>+</sup>CD43<sup>+</sup>SlgM<sup>-</sup>), generated by expression of *E2A-PBX1*<sup>17,39</sup>

or *Eu-RET* transgenes,<sup>18</sup> with the NP23 pro-B-1 ALL model. Hierarchical clustering clearly separated the murine pre-B-2 ALL and the NP23 pro-B-1 ALL samples (Figure 5A). We identified a gene set that was at least 2-fold overexpressed in pro-B-1 ALL compared with pre-B-2 ALL and used this gene signature in a GSEA comparison of human BCP-ALLs with *CRLF2* rearrangements (*CRLF2r*) with those without *CRLF2* rearrangements<sup>40</sup> (*RUNX1-ETV6* rearrangements and *CRLF2* rearrangements are mutually exclusive). As shown in Figure 5B, the murine pro-B-1 upregulated signature was strongly enriched in the *CRLF2r* group of patients.

Pro-B-1 lymphocytes have not yet been identified in humans, making it difficult to compare the immunophenotype of normal human pro-B-1 lymphocytes with that of patients with BCP-ALL and *CRLF2* rearrangement. However, mature human B-1 lymphocytes have a restricted V<sub>H</sub> region usage.<sup>10</sup> We reasoned that if patients with BCP-ALL and *CRLF2* activation showed the same preference for V<sub>H</sub> regions as did the mature human B-1 lymphocytes, that observation would further support the hypothesis that

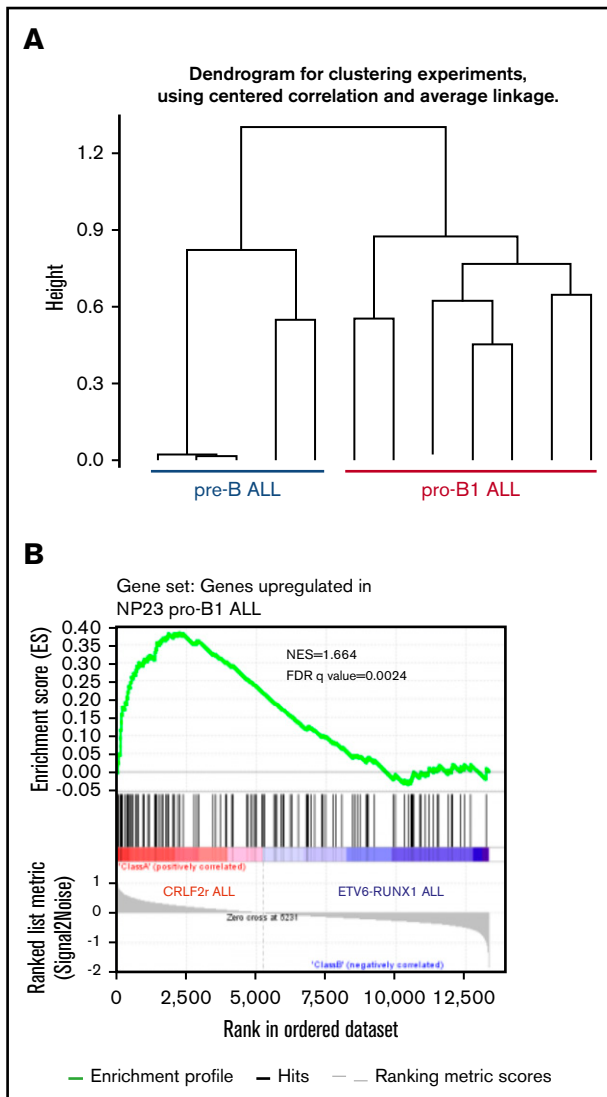


**Figure 5. NP23 pro-B-1 ALL gene signature is enriched in pediatric ALL with CRLF2 rearrangements.** (A) Hierarchical clustering of RNA-seq samples showing that NP23 pro-B-1 ALL expression profile is distinct from that of murine pre-B-2 ALL (taken from *E $\mu$ -RET* and *E2A-PBX* mice). (B) GSEA plot showing enrichment of NP23 pro-B-1 ALL gene signature in pediatric ALL carrying *CRLF2* rearrangements (GSE26281). The gene signature was generated by comparing NP23 pro-B-1 ALL with mouse pre-B-2 ALL (FPKM FC > 2).

a BCP-ALL with *CRLF2* activation is derived from pro-B-1 lymphocytes. We sequenced clonal *IGH* gene rearrangements from 23 patients with BCP-ALL and overexpression of *CRLF2* and from 28 patients from a genetically distinct group of BCP-ALLs (*ETV6-RUNX1*) that did not show *CRLF2* overexpression. Table 2 shows that 17 of the 23 patients with *CRLF2* overexpression used 1 of the B-1-preferred  $V_H$  gene regions (highlighted in red), whereas only 10 of 28 patients without *CRLF2* overexpression used 1 of these preferred V regions (2-tailed  $\chi^2 P = .0065$ ). In addition,  $V_H3-30$ , which was the most commonly used  $V_H$  region in mature human B-1 cells, accounting for >20% of the total,<sup>10</sup> was also the single most commonly used  $V_H$  region in patients with BCP-ALL and *CRLF2* overexpression, being used in 4 (17%) of

23 patients. Furthermore,  $V_H3-30$  and  $V_H3-74$ , the 2 most commonly used  $V_H$  regions in patients with *CRLF2*-overexpressing BCP-ALL (Table 2), are markedly overrepresented in the immune response to pneumococcal polysaccharides,<sup>41</sup> a response reported to be mediated by B-1 lymphocytes.

## Discussion

We have characterized a subset of NP23 transgenic mice that developed an aggressive, invasive leukemia with an immunophenotype (Lin<sup>-</sup>/B220<sup>-</sup>/CD19<sup>+</sup>/AA4.1<sup>+</sup>) that closely matched that of a pro-B-1 cell. Although similar to the BCP LBL described in the Bethesda proposals<sup>27</sup> for classifying murine lymphoid malignancy, these cells were B220<sup>-</sup> and thus were inconsistent with any known B-2 pro- or pre-B cell.<sup>20</sup> To the best of our knowledge, leukemias of pro-B-1 cells have not previously been described in mice or humans, and we designate these as pro-B-1 ALLs.

Gene expression profiling further supported the assertion that the NP23 B-lineage ALL arose from pro-B-1 cells. We used both gene expression arrays as well as RNA-seq to identify genes that were consistently upregulated in NP23 B-lineage ALL compared with WT B cells. Comparison of the genes most highly expressed in the pro-B-1 ALLs with gene expression profiles of murine B cells revealed that the NP23 pro-B-1 ALL was most similar to fetal liver pro-B fraction BC, more so than adult bone marrow pro-B fraction BC. Given that fetal liver fraction BC has been reported to be a source of B-1 B cells,<sup>22</sup> these observations again support a pro-B-1 cell as the normal counterpart of the NP23 B-lineage leukemias. Moreover, direct comparison of the genes most highly upregulated in NP23 pro-B-1 ALL with an independent RNA-seq data set revealed that the NP23-upregulated gene profile was more similar to that of pro-B-1 cells than pro-B-2 cells, further supporting the assertion that the NP23 B-lineage ALLs were of pro-B-1 origin.<sup>23</sup>

Clonality was evident by DJ or VDJ rearrangement in the B cells and demonstrated a bias toward the use of 3'  $V_H$  gene families  $V_H7183$  and  $V_HQ52$ , a phenomenon observed in fetal B-1 cells (reviewed by Montecino-Rodriguez and Dorshkind<sup>2</sup> and Hardy<sup>26</sup>), further supporting the pro-B-1-cell origin. Using the nomenclature and  $V_H$  family designation provided by ImMunoGeneTics, we noted that 10 of the 11  $V_H$  regions used belonged to the  $V_H1$ ,  $V_H2$ , or  $V_H5$  families; these 3 families made up >70% of  $V_H$  regions used by B-1a cells in 1 report.<sup>42</sup> Furthermore, use of the  $D_H$  segments DFL16.1, DSP, DST4, and DQ52 is characteristic of fetal B-1a cells<sup>42</sup>; Table 2 shows that all 13 of the clonal rearrangements used 1 of these 4 D segments. It should be noted that B-1 B cells have historically been thought to have little or no N region addition at VDJ junctions<sup>20,43</sup>; however, recent studies have clearly shown that subsets of pro-B-1 cells, specifically B-1a cells, have abundant N region addition.<sup>42,44</sup> In 1 study, B-1a cells derived from bone marrow CD19<sup>+</sup> cells showed N region addition,<sup>42</sup> and a second study demonstrated that the PC1<sup>10</sup> subset of B-1a cells had both frequent N region additions and preferential usage of the  $V_H5$  family.<sup>44</sup> Taken together, characteristics of *Igh* locus VDJ rearrangement further support the contention that these leukemias represent malignancies of pro-B-1 origin.

Remarkably, all 11 pro-B-1 ALL samples had acquired similar *Bcor* mutations during the process of transformation. All *Bcor* mutations were short indels, and all encoded a truncated form of the *Bcor* protein. *Bcor* was initially identified as a transcriptional corepressor



**Table 2. V<sub>H</sub> gene use in 2 genetic subgroups of patients with BCP-ALL**

Patient no.	IGH V region	Preferred B-1 V region?
<b>CRLF2 overexpression</b>		
360	IGHV3-74	+
365	IGHV3-23, IGHV3-49	+
379	IGHV3-74	+
400	IGHV3-33, IGHV3-30	+
552	IGHV1-3, IGHV3-11, IGHV3-33	
569	IGHV4-39	+
715	IGHV2-70	
802	IGHV4-34, IGHV3-30	+
833	IGHV4-39	+
839	IGHV3-71	
841	IGHV3-41, IGHV2-5	
873	IGHV4-61, IGHV3-66, IGHV1-69	+
887	IGHV3-74, IGHV2-70, IGHV1-69	+
903	IGHV1-8	
948	IGHV3-30	+
957	IGHV1-46, IGHV3-13, IGHV4-30	+
961	IGHV3-74, IGHV3-13	+
1047	IGHV4-39, IGHV3-7, IGHV2-26	+
1060	IGHV4-59	+
1063	IGHV3-71, IGHV3-30	+
1089	IGHV3-22, IGHV3-13	
1097	IGHV2-26	+
1101	IGHV3-9	+
<b>ETV6-RUNX1 fusion</b>		
960	IGHV3-21	
968	IGHV3-13	
985	IGHV3-23, IGHV2-5	+
991	IGHV6-1	
997	IGHV2-5, IGHV4-61	
999	IGHV3-22	
1000	IGHV3-15	
1029	IGHV5-3	
1034	IGHV1-2, IGHV1-2	+
1042	IGHV4-61, IGHV2-5, IGHV3-41	
1052	IGHV3-7	
1053	IGHV7-4, IGHV2-5, IGHV3-30	+
1054	IGHV1-2, IGHV2-5	+
1059	IGHV3-74	+
1061	IGHV3-53, IGHV1-69	+
1075	IGHV3-74	+
1081	IGHV3-13	
1084	IGHV1-8	
1115	IGHV1-69, IGHV4-55	+
1118	IGHV3-71, IGHV2-5	
1120	IGHV3-11, IGHV4-59	+
1122	IGHV2-70, IGHV3-23	+
1133	IGHV3-33	

**Table 2. (continued)**

Patient no.	IGH V region	Preferred B-1 V region?
1139	IGHV3-71, IGHV1-45	
1147	IGHV3-13	
1153	IGHV3-7	
1162	IGHV2-5	
1170	IGHV6-1	

of Bcl6<sup>45,46</sup> and interacts with a set of Polycomb group proteins to form a Polycomb repressor 1-like (PRC1-like) complex predicted to exert histone ubiquitylation and demethylation enzymatic functions.<sup>47,48</sup> Somatic frameshift and nonsense mutations of *BCOR* have previously been found to be distributed throughout the *BCOR* protein in AML,<sup>13</sup> bone sarcomas,<sup>49</sup> chronic myelomonocytic leukemia and myelodysplastic syndrome,<sup>14</sup> and pediatric rhabdomyosarcoma.<sup>50</sup> Because *BCOR* is X linked, and *BCOR* mutations are often frameshift mutations, it has been suggested that *BCOR* loss of function may provide a competitive advantage during malignant transformation. This hypothesis is supported by our failure to detect a truncated Bcor protein in the pro-B-1 samples. In addition, a recent report demonstrated an acquired *Bcor* frameshift mutation in a murine pre-B-2 ALL sample.<sup>51</sup> Alternatively, the observation that the *Bcor* mutations were tightly clustered in the pro-B-1 ALL samples might suggest that there is a specific gain of function conferred by a truncated Bcor protein that retains the Bcl6 interaction domain but lacks the ankyrin repeats and PUFD domain.

Eight of 11 pro-B-1 ALLs had acquired *Jak1/2/3* or *Stat5a* mutations, and all samples examined showed evidence of constitutive Stat signaling, based on increased pStat3 or pStat5. The combination of the *NP23* transgene along with spontaneous *Bcor* and *Jak* signaling pathway mutations in these pro-B-1 leukemias provides experimental support for a recently published model of high-risk ALL that was based on whole-genome sequencing of patients with BCP-ALL.<sup>52</sup> In this model, an initiating event leads to increased self-renewal of pro B cells, followed by a mutation that leads to a block in B-cell differentiation and a mutation that leads to increased proliferation. Experimental support for this model has recently been documented for pre-B-2 ALL but not pre-B-1 ALL.<sup>51,53</sup> In the case of *NP23* pro-B-1 ALL, the initial event leading to increased self-renewal is the *NP23* transgene, introduced into the mouse germline. Although *NP23* fusions are rare in B-lineage ALL, the *NP23* fusion leads to overexpression of *Hoxa* cluster genes, the overexpression of which is associated with increased stem-cell self-renewal.<sup>12,54</sup> The spontaneous, acquired mutations in *Bcor* and *Jak1/2* lead to a block in B-cell differentiation and hyperproliferation, respectively. This constellation of findings provides experimental support for a hypothesis in which mutations in 3 critical pathways, namely stem-cell self-renewal, impaired B-cell differentiation, and *Jak/Stat* cytokine signaling, collaborate to induce BCP-ALL.

There are interesting parallels between the pro-B-1 ALL that develops in *NP23* transgenic mice and *CRLF2*-associated BCP-ALL in humans, which represents ~5% of all childhood BCP-ALLs.<sup>37</sup> Both are associated with collaborative mutations in *JAK1* or *JAK2*, both show *CRLF2* overexpression (indeed, murine B-1 progenitors have been shown to be dependent on TSLP, which is the ligand for *CRLF2*), and the gene expression profile of murine

*NP23* pro-B-1 ALL is markedly more similar to that of *CRLF2r* ALL than non-*CRLF2r* ALL. Finally, both murine *NP23* pro-B-1 ALL and human *CRLF2r* ALL show preferential usage of a  $V_H$  region preferred by B-1 lymphocytes. Taken together, these findings lead to the intriguing hypothesis that patients with BCP ALL and *CRLF2* overexpression may have malignancies of pro-B-1 origin. We suggest that the *NP23* transgenic mouse will provide an important model for the study of B-1 B-cell development, as well as the molecular and genetic events that lead to pro-B-1 ALL.

## Acknowledgments

The authors thank Michael Kuehl, Andre Nussenzweig, Sandy Morse, Jack Shern, and current and former members of Aplan laboratory for insightful discussions. The authors also thank the National Cancer Institute (NCI) Sequencing Core for Sanger sequencing, the NCI Transgenic Core for generation of transgenic mice, Shelley Hoover and Mark Simpson of the NCI Molecular Pathology Unit for assistance with slide imaging, and Maria Jorge for excellent animal

husbandry and Vivian Bardwell for the kind gift of the anti-Bcor antibody.

This work was supported by the Intramural Research Program of the National Cancer Institute, National Institutes of Health (grant numbers ZIA SC 010378 and BC 010983).

## Authorship

Contribution: P.D.A., S.M.G., and L.G. conceived and designed the project; S.M.G., L.G., E.J., S.K., M.P., R.L.W., J.D., and S.F. performed experiments; S.M.G., L.G., Y.J.Z., S.B., Y.J.C., T.J.F., R.P.-G., P.S.M., and P.D.A. analyzed the data; all authors reviewed drafts of the manuscript; and P.D.A. wrote the final draft of the manuscript.

Conflict-of-interest disclosure: The authors declare no competing financial interests.

Correspondence: Peter D. Aplan, Genetics Branch, Center for Cancer Research, National Cancer Institute, National Institutes of Health, Building 37, 37 Convent Dr, Bethesda, MD 20892; e-mail: aplanp@mail.nih.gov.

## References

1. Swerdlow S, Campo E, Harris NL, et al, eds: WHO Classification of Tumours of Haematopoietic and Lymphoid Tissues. Lyon, France: IARC Press; 2008.
2. Montecino-Rodriguez E, Dorshkind K. B-1 B cell development in the fetus and adult. *Immunity*. 2012;36(1):13-21.
3. Barber CL, Montecino-Rodriguez E, Dorshkind K. Reduced production of B-1-specified common lymphoid progenitors results in diminished potential of adult marrow to generate B-1 cells. *Proc Natl Acad Sci USA*. 2011;108(33):13700-13704.
4. Montecino-Rodriguez E, Leathers H, Dorshkind K. Identification of a B-1 B cell-specified progenitor. *Nat Immunol*. 2006;7(3):293-301.
5. Griffin DO, Rothstein TL. Human b1 cell frequency: isolation and analysis of human b1 cells. *Front Immunol*. 2012;3:122.
6. Hardy RR. B-1 B cells: development, selection, natural autoantibody and leukemia. *Curr Opin Immunol*. 2006;18(5):547-555.
7. Shukla V, Ma S, Hardy RR, Joshi SS, Lu R. A role for IRF4 in the development of CLL. *Blood*. 2013;122(16):2848-2855.
8. Widhopf GF II, Brinson DC, Kipps TJ, Tighe H. Transgenic expression of a human polyreactive Ig expressed in chronic lymphocytic leukemia generates memory-type B cells that respond to nonspecific immune activation. *J Immunol*. 2004;172(4):2092-2099.
9. Pennell CA, Arnold LW, Lutz PM, LoCascio NJ, Willoughby PB, Haughton G. Cross-reactive idiotypes and common antigen binding specificities expressed by a series of murine B-cell lymphomas: etiological implications. *Proc Natl Acad Sci USA*. 1985;82(11):3799-3803.
10. Griffin DO, Rothstein TL. A small CD11b(+) human B1 cell subpopulation stimulates T cells and is expanded in lupus. *J Exp Med*. 2011;208(13):2591-2598.
11. Montecino-Rodriguez E, Li K, Fice M, Dorshkind K. Murine B-1 B cell progenitors initiate B-acute lymphoblastic leukemia with features of high-risk disease. *J Immunol*. 2014;192(11):5171-5178.
12. Gough SM, Lee F, Yang F, et al. NUP98-PHF23 is a chromatin-modifying oncoprotein that causes a wide array of leukemias sensitive to inhibition of PHD histone reader function. *Cancer Discov*. 2014;4(5):564-577.
13. Grossmann V, Tiacci E, Holmes AB, et al. Whole-exome sequencing identifies somatic mutations of BCOR in acute myeloid leukemia with normal karyotype. *Blood*. 2011;118(23):6153-6163.
14. Damm F, Chesnais V, Nagata Y, et al. BCOR and BCORL1 mutations in myelodysplastic syndromes and related disorders. *Blood*. 2013;122(18):3169-3177.
15. Den Boer ML, van Slegtenhorst M, De Menezes RX, et al. A subtype of childhood acute lymphoblastic leukaemia with poor treatment outcome: a genome-wide classification study. *Lancet Oncol*. 2009;10(2):125-134.
16. Harvey RC, Mullighan CG, Wang X, et al. Identification of novel cluster groups in pediatric high-risk B-precursor acute lymphoblastic leukemia with gene expression profiling: correlation with genome-wide DNA copy number alterations, clinical characteristics, and outcome. *Blood*. 2010;116(23):4874-4884.
17. Bijl J, Sauvageau M, Thompson A, Sauvageau G. High incidence of proviral integrations in the Hoxa locus in a new model of E2a-PBX1-induced B-cell leukemia. *Genes Dev*. 2005;19(2):224-233.
18. Zeng XX, Zhang H, Hardy RR, Wasserman R. The fetal origin of B-precursor leukemia in the E-mu-ret mouse. *Blood*. 1998;92(10):3529-3536.
19. Ogilvy S, Metcalf D, Gibson L, Bath ML, Harris AW, Adams JM. Promoter elements of *vav* drive transgene expression in vivo throughout the hematopoietic compartment. *Blood*. 1999;94(6):1855-1863.
20. Hardy RR, Hayakawa K. B cell development pathways. *Annu Rev Immunol*. 2001;19:595-621.
21. Trowbridge IS, Thomas ML. CD45: an emerging role as a protein tyrosine phosphatase required for lymphocyte activation and development. *Annu Rev Immunol*. 1994;12:85-116.

22. Zhou Y, Li YS, Bandi SR, et al. Lin28b promotes fetal B lymphopoiesis through the transcription factor Arid3a. *J Exp Med*. 2015;212(4):569-580.
23. Montecino-Rodriguez E, Fice M, Casero D, Berent-Maoz B, Barber CL, Dorshkind K. Distinct genetic networks orchestrate the emergence of specific waves of fetal and adult B-1 and B-2 development. *Immunity*. 2016;45(3):527-539.
24. Johnston CM, Wood AL, Bolland DJ, Corcoran AE. Complete sequence assembly and characterization of the C57BL/6 mouse Ig heavy chain V region. *J Immunol*. 2006;176(7):4221-4234.
25. Ye J. The immunoglobulin IGHD gene locus in C57BL/6 mice. *Immunogenetics*. 2004;56(6):399-404.
26. Hardy RR. B-1 B cell development. *J Immunol*. 2006;177(5):2749-2754.
27. Morse HC III, Anver MR, Fredrickson TN, et al; Hematopathology subcommittee of the Mouse Models of Human Cancers Consortium. Bethesda proposals for classification of lymphoid neoplasms in mice. *Blood*. 2002;100(1):246-258.
28. Goldberg L, Gough SM, Lee F, et al. Somatic mutations in murine models of leukemia and lymphoma: Disease specificity and clinical relevance. *Genes Chromosomes Cancer*. 2017;56(6):472-483.
29. Babon JJ, Lucet IS, Murphy JM, Nicola NA, Varghese LN. The molecular regulation of Janus kinase (JAK) activation. *Biochem J*. 2014;462(1):1-13.
30. Zhang J, Mullighan CG, Harvey RC, et al. Key pathways are frequently mutated in high-risk childhood acute lymphoblastic leukemia: a report from the Children's Oncology Group. *Blood*. 2011;118(11):3080-3087.
31. Loh ML, Zhang J, Harvey RC, et al. Tyrosine kinome sequencing of pediatric acute lymphoblastic leukemia: a report from the Children's Oncology Group TARGET Project. *Blood*. 2013;121(3):485-488.
32. Mullighan CG, Zhang J, Harvey RC, et al. JAK mutations in high-risk childhood acute lymphoblastic leukemia. *Proc Natl Acad Sci USA*. 2009;106(23):9414-9418.
33. Asnafi V, Le Noir S, Lhermitte L, et al. JAK1 mutations are not frequent events in adult T-ALL: a GRAALL study. *Br J Haematol*. 2010;148(1):178-179.
34. Porcu M, Kleppe M, Gianfelici V, et al. Mutation of the receptor tyrosine phosphatase PTPRC (CD45) in T-cell acute lymphoblastic leukemia. *Blood*. 2012;119(19):4476-4479.
35. Staerk J, Kallin A, Demoulin JB, Vainchenker W, Constantinescu SN. JAK1 and Tyk2 activation by the homologous polycythemia vera JAK2 V617F mutation: cross-talk with IGF1 receptor. *J Biol Chem*. 2005;280(51):41893-41899.
36. Vainchenker W, Constantinescu SN. JAK/STAT signaling in hematological malignancies. *Oncogene*. 2013;32(21):2601-2613.
37. Izraeli S. Beyond Philadelphia: 'Ph-like' B cell precursor acute lymphoblastic leukemias—diagnostic challenges and therapeutic promises. *Curr Opin Hematol*. 2014;21(4):289-296.
38. Tasian SK, Doral MY, Borowitz MJ, et al. Aberrant STAT5 and PI3K/mTOR pathway signaling occurs in human CRLF2-rearranged B-precursor acute lymphoblastic leukemia. *Blood*. 2012;120(4):833-842.
39. Jacoby E, Nguyen SM, Fountaine TJ, et al. CD19 CAR immune pressure induces B-precursor acute lymphoblastic leukaemia lineage switch exposing inherent leukaemic plasticity. *Nat Commun*. 2016;7:12320.
40. Figueroa ME, Chen SC, Andersson AK, et al. Integrated genetic and epigenetic analysis of childhood acute lymphoblastic leukemia. *J Clin Invest*. 2013;123(7):3099-3111.
41. Kolibab K, Smithson SL, Rabquer B, Khuder S, Westerink MA. Immune response to pneumococcal polysaccharides 4 and 14 in elderly and young adults: analysis of the variable heavy chain repertoire. *Infect Immun*. 2005;73(11):7465-7476.
42. Holodick NE, Vizconde T, Rothstein TL. B-1a cell diversity: nontemplated addition in B-1a cell Ig is determined by progenitor population and developmental location. *J Immunol*. 2014;192(5):2432-2441.
43. Feeney AJ. Lack of N regions in fetal and neonatal mouse immunoglobulin V-D-J junctional sequences. *J Exp Med*. 1990;172(5):1377-1390.
44. Wang H, Shin DM, Abbasi S, et al. Expression of plasma cell alloantigen 1 defines layered development of B-1a B-cell subsets with distinct innate-like functions. *Proc Natl Acad Sci USA*. 2012;109(49):20077-20082.
45. Fukuda T, Yoshida T, Okada S, et al. Disruption of the Bcl6 gene results in an impaired germinal center formation. *J Exp Med*. 1997;186(3):439-448.
46. Ghetu AF, Corcoran CM, Cerchiotti L, Bardwell VJ, Melnick A, Privé GG. Structure of a BCOR corepressor peptide in complex with the BCL6 BTB domain dimer. *Mol Cell*. 2008;29(3):384-391.
47. Gearhart MD, Corcoran CM, Wamstad JA, Bardwell VJ. Polycomb group and SCF ubiquitin ligases are found in a novel BCOR complex that is recruited to BCL6 targets. *Mol Cell Biol*. 2006;26(18):6880-6889.
48. Junco SE, Wang R, Gaipa JC, et al. Structure of the polycomb group protein PCGF1 in complex with BCOR reveals basis for binding selectivity of PCGF homologs. *Structure*. 2013;21(4):665-671.
49. Pierron G, Tirode F, Lucchesi C, et al. A new subtype of bone sarcoma defined by BCOR-CCNB3 gene fusion. *Nat Genet*. 2012;44(4):461-466.
50. Shern JF, Chen L, Chmielecki J, et al. Comprehensive genomic analysis of rhabdomyosarcoma reveals a landscape of alterations affecting a common genetic axis in fusion-positive and fusion-negative tumors. *Cancer Discov*. 2014;4(2):216-231.
51. Duque-Afonso J, Feng J, Scherer F, et al. Comparative genomics reveals multistep pathogenesis of E2A-PBX1 acute lymphoblastic leukemia. *J Clin Invest*. 2015;125(9):3667-3680.
52. Hunger SP, Mullighan CG. Redefining ALL classification: toward detecting high-risk ALL and implementing precision medicine. *Blood*. 2015;125(26):3977-3987.
53. Fry TJ, Aplan PD. A robust in vivo model for B cell precursor acute lymphoblastic leukemia. *J Clin Invest*. 2015;125(9):3427-3429.
54. Wu M, Kwon HY, Rattis F, et al. Imaging hematopoietic precursor division in real time. *Cell Stem Cell*. 2007;1(5):541-554.